Applied Physics Letters

RESEARCH ARTICLE | SEPTEMBER 25 2023

Superconducting nanowire single photon detector on 4H-SiC substrates with saturated quantum efficiency

Mengting Si ; Liping Zhou; Wei Peng ; Xingyu Zhang ; Ailun Yi ; Chengli Wang; Hourong Zhou; Zhen Wang; Xin Ou ; Lixing You

Appl. Phys. Lett. 123, 131106 (2023)
https://doi.org/10.1063/5.0164368

Applied Physics Letters ARTICLE pubs.aip.org/aip/apl

Superconducting nanowire single photon detector on 4H-SiC substrates with saturated quantum efficiency

Cite as: Appl. Phys. Lett. **123**, 131106 (2023); doi: 10.1063/5.0164368
Submitted: 12 July 2023 · Accepted: 7 September 2023 ·
Published Online: 25 September 2023

Mengting Si,[1,2] Liping Zhou,[1,3] Wei Peng,[1,4] Xingyu Zhang,[1,4] Ailun Yi,[1] Chengli Wang,[1] Hourong Zhou,[1] Zhen Wang,[1,3,4] Xin Ou,[1,3,a)] and Lixing You[1,3,4,a)]

AFFILIATIONS

[1]National Key Laboratory of Materials for Integrated Circuits, Shanghai Institute of Microsystem and Information Technology, Chinese Academy of Sciences, Shanghai, China
[2]School of Physics, Peking University, Beijing, China
[3]Center of Materials Science and Optoelectronics Engineering, University of Chinese Academy of Sciences, Beijing, China
[4]CAS Center for Excellence in Superconducting Electronics (CENSE), Shanghai, China

[a)]**Authors to whom correspondence should be addressed:** ouxin@mail.sim.ac.cn and lxyou@mail.sim.ac.cn

ABSTRACT

On-chip single photon detection is crucial for implementing on-chip quantum communication, quantum simulation, and calculation. Superconducting nanowire single-photon detectors (SNSPDs) have become one of the essential techniques to achieve high-efficiency, on-chip, single-photon detection at scale due to their high detection efficiency, low dark count rate, and low jitter. Silicon carbide (SiC) has emerged as a promising integrated photonics platform due to its nonlinear optical processing capabilities, compatibility with CMOS technology, and outstanding quantum properties as a device for single photon sources. However, achieving high-efficiency superconducting nanowire single-photon detection on SiC substrates has yet to be demonstrated. In this study, we deposited polycrystalline NbN thin films onto 4H-SiC substrates. We also ensured that the deposited NbN thin film had a flat surface with a roughness less than 1 nm on the C-side 4H-SiC substrate through optimized chemical mechanical polishing. The NbN-SNSPD achieved a saturated quantum efficiency covering the color center emission bandwidth wavelength range (from 861 to 1550 nm) of the 4H-SiC material. These results offer a promising solution for high-efficiency single-photon detection on fully integrated quantum optical chips on 4H-SiC substrates.

Solid-state qubit candidates with defects, such as diamond,[1,2] silicon carbide,[3–6] and rare earth ions material,[7] are emerging as promising platforms for quantum memory,[8,9] quantum computation,[10,11] quantum communication,[12,13] and quantum information processing.[14] Among them, silicon carbide is drawing increasing attention due to its outstanding optical properties,[15] such as nonlinear optical properties,[16,17] mature crystal growth technique,[18,19] and good compatibility and scalability with complementary metal–oxide–semiconductor fabrication process.[20,21] Silicon carbide has numerous polytypes and various types of defects. 4H-SiC defects possess long emission time,[15] long-lived electron spin coherence time,[22–24] and high readout ratio.[25] To date, studies on the fabrication of 4H-SiC-on-insulator substrates (4H-SiCOI),[26] addressable implanted color centers near the surface of 4H-SiC,[27,28] and devices, such as micro rings,[29] cavities photonics crystals,[30,31] frequency combs,[32] and solitons,[33] have been carried out. These achievements present the possibility for complex integration and applications on 4H-SiC. Therefore, it is viewed as a potential integrated photonics platform. However, single photon detection for color centers on 4H-SiC has yet been carried out, despite being an important element for fully integrated photonics quantum chips.

Superconducting nanowire single photon detectors (SNSPDs), normally based on silicon substrates, offer high detection efficiency,[34,35] low dark count rate, low timing jitter,[36] and wide bandwidth from x-ray[37] to mid-infrared range.[38,39] Currently, SNSPDs can be integrated on various substrate materials, such as X-cut lithium niobate (LN),[40,41] silicon,[42] and silicon nitride[43,44] with intrinsic detection efficiency near 100% at 1550 nm and shorter wavelength. On silicon carbides, SNSPDs have been fabricated on 3C-SiC. The detector

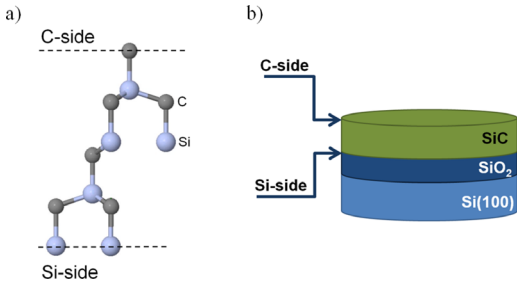

FIG. 1. (a) The crystal structure of 4H-SiC. (b) The structure of 4H-SiCOI substrates. The upper surface is C-side.

showed a single photon response with a moderate unsaturated device detection efficiency of around 20%.[45] The detection efficiency may be affected by the structures of NbN thin films. NbN thin films deposited on 3C-SiC[46] and 4H-SiC[47] substrates are epitaxial due to slight lattice mismatch. Previous research suggests that polycrystalline thin films are more likely to induce better performance in SNSPDs than epitaxial films.[41]

In this research, the natural oxide layer of 4H-SiC was retained to prevent NbN thin films from epitaxial growth on 4H-SiC substrates. Following the popular fabrication processes of NbN-SNSPD on the Si substrate, we obtained an NbN-SNSPD on 4H-SiC with broadband saturated detection. The results demonstrate the possibility of on-chip high-efficiency single-photon detection on 4H-SiC materials as integrated platforms.

Due to its spontaneous polarization, 4H-SiC has two sides, as shown in Fig. 1(a). Si-side is usually used in the binding process of 4H-SiCOI fabrication, as shown in Fig. 1(b), which makes the upper surface the C-side of the SiCOI substrate. We chose to fabricate NbN thin films and SNSPDs on the C-side. 4H-SiC substrates have a size of $20 \times 22\ mm^2$. Using an optimized chemical mechanical polishing process, the root mean square surface roughness (R_q) was reduced to lower than 0.2 nm.

NbN thin films (3–200 nm) were fabricated using DC magnetron sputtering. The detailed deposition parameter and the process are the same as the previous study on the deposition of NbN thin films onto the silicon substrate.[35] We measured the superconducting properties of NbN thin films using a physical properties measurement system, while topography and surface roughness were analyzed by atomic force microscopy (AFM). The crystal structure was detected by x-ray diffraction (XRD). The device was fabricated using processes such as electron beam lithography and reactive ion etching. After dicing, the device was mounted in a custom-made copper holder and electrically connected using wire bonding. The optical fiber was coupled to the device's photosensitive area using a vertical coupling method. Device measurements and characterizations, such as I–V characterization, system detection efficiency, and jitter characterization, were performed. The methods and equipment details can be referred to in our previous paper.[35]

Figure 2(a) displays the topography of an 8-nm-thick NbN thin film on a 4H-SiC substrate. Randomly oriented trenches were brought by the morphology of the surface of the C-side 4H-SiC substrate. The R_q value of the NbN thin film was 0.37 nm within a scanning range of $5 \times 5\ \mu m^2$, satisfying the fabrication requirement for SNSPDs. Figure 2(b) is the scanning electron microscopy (SEM) image of the photoreactive area of an NbN-SNSPD device, with the inset providing measurements of the detector's width and pitch. The detector is circular with a diameter of 15 μm, while the nanowire has a width of 62 nm and the pitch is 162 nm.

Figure 3(a) shows the superconducting transition of a 6-nm-thick NbN thin film deposited on the C side of the 4H-SiC substrate. The transition temperature (T_c) was determined as the temperature at which the thin film's resistance reaches half its value before the transition. The transition width (ΔT_c) was calculated as the temperature range between 90% and 10% of the resistance before the transitions. The 6-nm-thick NbN thin film exhibited a T_c of 6.7 K and a ΔT_c of 0.4 K. Figure 3(b) illustrates the dependence of the T_c and ΔT_c on film thickness, ranging from 6 to 200 nm. As the thin film thickness increased, T_c increased and ΔT_c decreased. A 200-nm-thick NbN film exhibited a T_c of 16 K and a ΔT_c of 0.1 K. The value of residual resistance ratio (RRR) was defined as the resistance at 300 K over the resistance at 20 K. The RRR values were 0.6 and 0.8 for a 6- and 200-nm-thick films, respectively. The higher RRR value for thicker films corresponded with the results of T_c and ΔT_c. As the thin film thickness increased, it demonstrated better superconducting properties with a higher T_c approaching 16 K. Additionally, the ΔT_c decreased to as low as 0.1 K, indicating that the depositions were close to the optimal deposition parameters with approximately a 1:1 stoichiometric ratio. Therefore, the low T_c observed at the beginning of the growth was not due to deviation from stoichiometry but relatively low crystallinity. Figure 3(c) compares the dependence of T_c values on NbN film thickness on various substrates, including MgO, X-cut, Z-cut, and 4H-SiC substrates.[41] Previous research has shown that NbN thin films are single crystalline, epitaxial with dense twins, and polycrystalline on MgO, Z-cut LN, and X-cut LN substrates, respectively.[41,47]

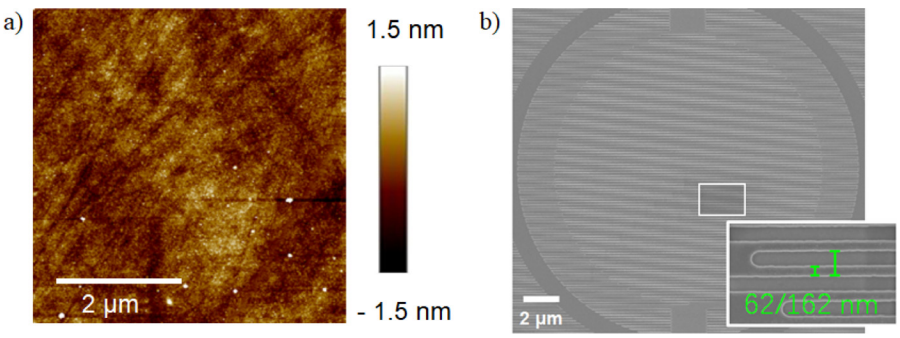

FIG. 2. (a) AFM characterization of 8-nm-think NbN film. (b) The SEM image of the fabricated NbN-SNSPD device in this paper. The inset shows the width and pitch of the nanowire.

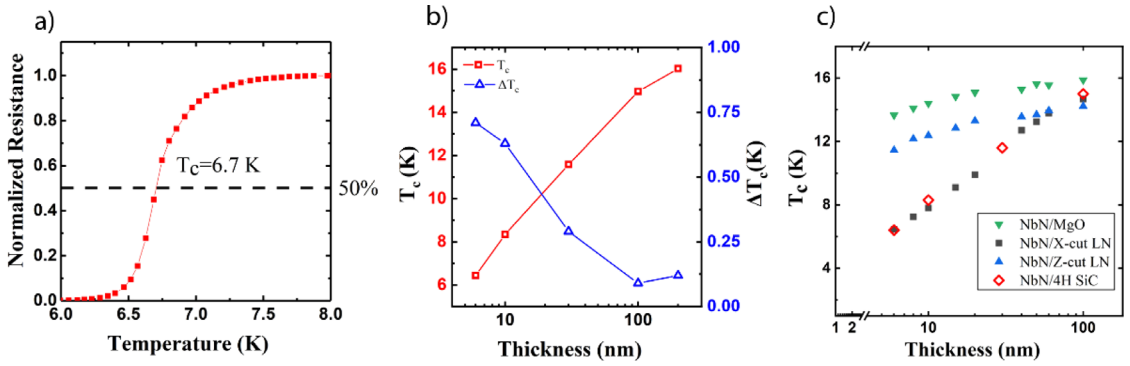

FIG. 3. (a) Dependence of normalized resistance on temperatures of a 6-nm-thick NbN thin film. (b) The T_c and ΔT_c of NbN thin films with thicknesses from 6 to 200 nm. (c) The relationships of the transition temperatures and thickness of NbN thin film on MgO (down triangle), X-cut LN (square), Z-cut LN (up triangle), and 4H-SiC substrates (hollow diamond).

The T_c-thickness dependence of NbN thin films on 4H-SiC substrates is more similar to that of polycrystalline NbN thin films, which were grown on Si and X-cut LN substrates, meanwhile different from those of epitaxial NbN thin films on MgO and Z-cut LN substrates. The XRD result shows two peaks of NbN materials, verifying the polycrystalline structure (see Fig. S1 in the supplementary material). Given that NbN deposition reaches a balanced stoichiometric ratio, the difference in NbN crystal structures was mainly caused by the degree of lattice mismatch with substrate materials.

The device's electrical characteristics, single-photon response, and jitter properties were tested under an environment with a power level of −108.92 dBm. Figure 4(a) illustrates the I–V characterization of the device, indicating a critical current of 9.1 μA and a corresponding critical current density of 2 MA/cm^2 at a temperature of 2.2 K. Figure 4(b) shows the dependency of normalized system detection efficiency (SDE) and dark count rate on bias current at 861, 1064, and 1550 nm wavelength. The respective absolute SDE values are 1.1%, 1.5%, and 1.2%. The device detected single photons with saturated efficiency and a low dark count rate. Figure 4(c) shows the device's single photon response signal with a response time (dead time) of 34 ns simulated for the falling part (1/e criterion). Figure 4(d) demonstrates the jitter characterization of the device in the 1064 and 1550 nm wavelengths with jitters of 106 and 111 ps, respectively. Upon on-chip integration, jitters are expected to decrease significantly due to the shortened nanowire length.

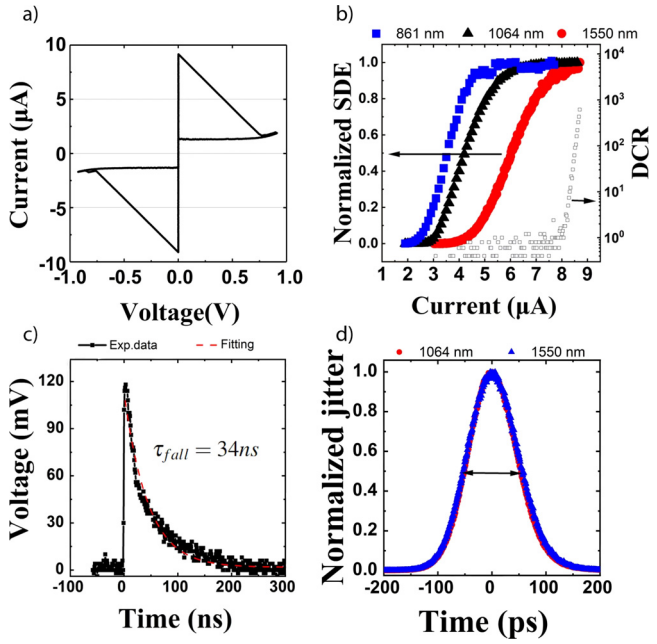

FIG. 4. (a) I–V curves, (b) system detection efficiency (left) and dark count rate (right) vs bias current, (c) oscilloscope persistence map of a response, and (d) jitters characterization of NbN-SNSPD on 4H-SiC substrates.

In Ref. 47, it reported that a 5-nm-thick NbN thin film on 4H-SiC substrate processes a T_c of 11 K,[47] which differs from our results. This discrepancy can be attributed to using of HF solution to remove the oxide layer of 4H-SiC substrates, which resulted in the epitaxial growth of NbN on the substrate. Additionally, due to the slight lattice mismatch, NbN thin films grown on 3C-SiC exhibit higher T_c values, and the detectors demonstrate unsaturated detection.[45] In contrast, in our research, we chose to retain the oxide layer, resulting in polycrystalline NbN structures, lower T_c values, and saturated detection behavior of detectors.

Based on our research on NbN thin film on LN substrate, epitaxial NbN thin films contribute less to the high performance of SNSPD than polycrystalline NbN thin films.[41] The results of our device are consistent with this conclusion. Here, the device performance is more similar to and comparable with the results of NbN-SNSPDs on Si substrates, indicating high device detection efficiency of on-chip waveguide integrated NbN-SNSPD on 4H-SiC photonics chips once the evanescent field absorption efficiency be enhanced. These results help to further integrate of high-efficiency on-chip SNSPDs on 4H-SiCOI substrates.

In conclusion, our study has demonstrated that NbN thin films with thicknesses ranging from 6 to 200 nm can be deposited on the C-side of 4H-SiC substrates. The relationship between the thickness of NbN thin films and their transition temperature follows the regular pattern of polycrystalline NbN thin films. Our fabricated NbN-SNSPD device with a width of 62 nm exhibits a critical temperature of up to

9.1 μA. It shows saturated quantum detection efficiency at 861, 1064, and 1550 nm wavelengths, with a low dark count rate. These results support the further exploration of high-performance integrated NbN-SNSPDs on 4H-SiC and 4H-SiCOI photonics chips, which could have significant implications for future research in the field of photonics. Specifically, the high critical temperature and quantum detection efficiency of our NbN-SNSPD device could enable new types of experiments or applications, such as single-photon characterization and manipulation, with potential applications in quantum information processing and communication.

See the supplementary material for the x-ray diffraction characterization result of a 200-nm-thick NbN film grown on 4H-SiC substrate.

The devices were fabricated at Superconducting Electronics Facility (SELF) of SIMIT.

AUTHOR DECLARATIONS

Conflict of Interest

The authors have no conflicts to disclose.

Author Contributions

Mengting Si: Conceptualization (lead); Formal analysis (lead); Investigation (lead); Project administration (lead); Writing – original draft (lead). **Lixing You:** Resources (equal); Supervision (equal); Validation (equal); Writing – review & editing (equal). **Liping Zhou:** Investigation (equal). **Wei Peng:** Formal analysis (lead); Validation (equal); Writing – review & editing (equal). **Xingyu Zhang:** Investigation (equal); Validation (equal). **Ailun Yi:** Validation (equal); Writing – review & editing (equal). **Chengli Wang:** Conceptualization (equal). **Hourong Zhou:** Investigation (supporting). **Zhen Wang:** Resources (equal). **Xin Ou:** Resources (equal).

DATA AVAILABILITY

The data that support the findings of this study are available from the corresponding author upon reasonable request.

REFERENCES

[1]J. R. Weber, W. F. Koehl, J. B. Varley, A. Janotti, B. B. Buckley, C. G. Van De Walle, and D. D. Awschalom, "Quantum computing with defects," Proc. Natl. Acad. Sci. U. S. A. **107**(19), 8513–8518 (2010).
[2]I. Aharonovich, A. D. Greentree, and S. Prawer, "Diamond photonics," Nat. Photonics **5**(7), 397–405 (2011).
[3]G. Wolfowicz, C. P. Anderson, B. Diler, O. G. Poluektov, F. J. Heremans, and D. D. Awschalom, "Vanadium spin qubits as telecom quantum emitters in silicon carbide," Sci. Adv. **6**(18), eaaz1192 (2020).
[4]W. F. Koehl, B. B. Buckley, F. J. Heremans, G. Calusine, and D. D. Awschalom, "Room temperature coherent control of defect spin qubits in silicon carbide," Nature **479**(7371), 84–87 (2011).
[5]Q. Li, J. Y. Zhou, Z. H. Liu, J. S. Xu, C. F. Li, and G. C. Guo, "Stable single photon sources in the near C-band range above 400 K," J. Semicond. **40**(7), 072902 (2019).
[6]L. Spindlberger, A. Csóré, G. Thiering, S. Putz, R. Karhu, J. U. Hassan, N. T. Son, T. Fromherz, A. Gali, and M. Trupke, "Optical properties of vanadium in 4 H silicon carbide for quantum technology," Phys. Rev. Appl. **12**(1), 014015 (2019).
[7]M. Zhong, M. P. Hedges, R. L. Ahlefeldt, J. G. Bartholomew, S. E. Beavan, S. M. Wittig, J. J. Longdell, and M. J. Sellars, "Optically addressable nuclear spins in a solid with a six-hour coherence time," Nature **517**(7533), 177–180 (2015).
[8]D. M. Lukin, M. A. Guidry, and J. Vučković, "Integrated quantum photonics with silicon carbide: challenges and prospects," PRX Quantum **1**(2), 020102 (2020).
[9]B. Tissot, M. Trupke, P. Koller, T. Astner, and G. Burkard, "Nuclear spin quantum memory in silicon carbide," Phys. Rev. Res. **4**(3), 033107 (2022).
[10]J. P. Philbin and P. Narang, "Computational materials insights into solid-state multiqubit systems," PRX Quantum **2**(3), 030102 (2021).
[11]I. D'Amico, D. G. Angelakis, F. Bussières, H. Caglayan, C. Couteau, T. Durt, B. Kolaric, P. Maletinsky, W. Pfeiffer, P. Rabl, A. Xuereb, and M. Agio, "Nanoscale quantum optics," Riv. Nuovo Cimento **42**, 153–195 (2019).
[12]M. Atatüre, D. Englund, N. Vamivakas, S. Lee, and J. Wrachtrup, "Material platforms for spin-based photonic quantum technologies," Nat. Rev. Mater. **3**(5), 38–51 (2018).
[13]N. Morioka, C. Babin, R. Nagy, I. Gediz, E. Hesselmeier, D. Liu, M. Joliffe, M. Niethammer, D. Dasari, V. Vorobyov, R. Kolesov, R. Stöhr, J. Ul-Hassan, N. T. Son, T. Ohshima, P. Udvarhelyi, G. Thiering, A. Gali, J. Wrachtrup, and F. Kaiser, "Spin-controlled generation of indistinguishable and distinguishable photons from silicon vacancy centres in silicon carbide," Nat. Commun. **11**, 2516 (2020).
[14]L. P. Yang, C. Burk, M. Widmann, S. Y. Lee, J. Wrachtrup, and N. Zhao, "Electron spin decoherence in silicon carbide nuclear spin bath," Phys. Rev. B. **90**(24), 241203 (2014).
[15]A. Lohrmann, B. C. Johnson, J. C. McCallum, and S. Castelletto, "A review on single photon sources in silicon carbide," Rep. Prog. Phys. **80**(3), 034502 (2017).
[16]S. Castelletto, A. Peruzzo, C. Bonato, B. C. Johnson, M. Radulaski, H. Ou, F. Kaiser, and J. Wrachtrup, "Silicon carbide photonics bridging quantum technology," ACS Photonics **9**(5), 1434–1457 (2022).
[17]A. Yi, C. Wang, L. Zhou, Y. Zhu, S. Zhang, T. You, J. Zhang, and X. Ou, "Silicon carbide for integrated photonics," Appl. Phys. Rev. **9**(3), 031302 (2022).
[18]S. Majety, P. Saha, V. A. Norman, and M. Radulaski, "Quantum information processing with integrated silicon carbide photonics," J. Appl. Phys. **131**(13), 130901 (2022).
[19]G. Moody, V. J. Sorger, D. J. Blumenthal, P. W. Juodawlkis, W. Loh, C. Sorace-Agaskar, A. E. Jones, K. C. Balram, J. C. F. Matthews, A. Laing, M. Davanco, L. Chang, J. E. Bowers, N. Quack, C. Galland, I. Aharonovich, M. A. Wolff, C. Schuck, N. Sinclair, M. Lončar, T. Komljenovic, D. Weld, S. Mookherjea, S. Buckley, M. Radulaski, S. Reitzenstein, B. Pingault, B. Machielse, D. Mukhopadhyay, A. Akimov, A. Zheltikov, G. S. Agarwal, K. Srinivasan, J. Lu, H. X. Tang, W. Jiang, T. P. McKenna, A. H. Safavi-Naeini, S. Steinhauer, A. W. Elshaari, V. Zwiller, P. S. Davids, N. Martinez, M. Gehl, J. Chiaverini, K. K. Mehta, J. Romero, N. B. Lingaraju, A. M. Weiner, D. Peace, R. Cernansky, M. Lobino, E. Diamanti, L. T. Vidarte, and R. M. Camacho, "2022 Roadmap on integrated quantum photonics," J. Phys. Photonics **4**(1), 012501 (2022).
[20]D. Lukin, C. Dory, M. Radulaski, S. Sun, S. D. Mishra, M. Guidry, D. Vercruysse, and J. Vuckovic, "4H-SiC-on-insulator platform for quantum photonics," in *Conference on Lasers and Electro-Optics* (IEEE, 2019).
[21]Y. Ailun, *Fabrication of 4H-SiC-on-Insulator Platform and Its Applications* (University of Chinese Academy of Sciences, 2021).
[22]D. J. Christle, P. V. Klimov, C. F. de las Casas, K. Szász, V. Ivády, V. Jokubavicius, J. U. Hassan, M. Syväjärvi, W. F. Koehl, T. Ohshima, N. T. Son, E. Janzén, Á. Gali, and D. D. Awschalom, "Isolated spin qubits in SiC with a high-fidelity infrared spin-to-photon interface," Phys. Rev. X **7**(2), 021046 (2017).
[23]D. J. Christle, A. L. Falk, P. Andrich, P. V. Klimov, J. U. Hassan, N. T. Son, E. Janzén, T. Ohshima, and D. D. Awschalom, "Isolated electron spins in silicon carbide with millisecond coherence times," Nat. Mater. **14**, 160–163 (2015).
[24]H. Seo, A. L. Falk, P. V. Klimov, K. C. Miao, G. Galli, and D. D. Awschalom, "Quantum decoherence dynamics of divacancy spins in silicon carbide," Nat. Commun. **7**, 12935 (2016).
[25]Q. Li, J.-F. Wang, F.-F. Yan, J.-Y. Zhou, H.-F. Wang, H. Liu, L.-P. Guo, X. Zhou, A. Gali, Z.-H. Liu, Z.-Q. Wang, K. Sun, G.-P. Guo, J.-S. Tang, H. Li, L.-X. You, J.-S. Xu, C.-F. Li, and G.-C. Guo, "Room-temperature coherent manipulation of single-spin qubits in silicon carbide with a high readout contrast," Natl. Sci. Rev. **9**(5), 85–94 (2022).

[26]A. Yi, Y. Zheng, H. Huang, J. Lin, Y. Yan, T. You, K. Huang, S. Zhang, C. Shen, M. Zhou, W. Huang, J. Zhang, S. Zhou, H. Ou, and X. Ou, "Wafer-scale 4H-silicon carbide-on-insulator (4H-SiCOI) platform for nonlinear integrated optical devices," Opt. Mater. (Amst.) **107**, 109990 (2020).
[27]Q. Li, J. F. Wang, F. F. Yan, Z. Di Cheng, Z. H. Liu, K. Zhou, L. P. Guo, X. Zhou, W. P. Zhang, X. X. Wang, W. Huang, J. S. Xu, C. F. Li, and G. C. Guo, "Nanoscale depth control of implanted shallow silicon vacancies in silicon carbide," Nanoscale **11**(43), 20554–20561 (2019).
[28]F. F. Yan, A. L. Yi, J. F. Wang, Q. Li, P. Yu, J. X. Zhang, A. Gali, Y. Wang, J. S. Xu, X. Ou, C. F. Li, and G. C. Guo, "Room-temperature coherent control of implanted defect spins in silicon carbide," npj Quantum Inf. **6**(1), 38 (2020).
[29]Y. Zheng, M. Pu, A. Yi, X. Ou, and H. Ou, "4H-SiC microring resonators for nonlinear integrated photonics," Opt. Lett. **44**(23), 5784–5787 (2019).
[30]B.-S. Song, T. Asano, S. Jeon, H. Kim, C. Chen, D. D. Kang, and S. Noda, "Ultrahigh-Q photonic crystal nanocavities based on 4H silicon carbide," Optica **6**(8), 991–995 (2019).
[31]L. Zhou, C. Wang, A. Yi, C. Shen, Y. Zhu, K. Huang, M. Zhou, J. Zhang, and X. Ou, "Photonic crystal nanobeam cavities based on 4H-silicon carbide on insulator," Chin. Opt. Lett. **20**(3), 031302 (2022).
[32]C. Wang, Z. Fang, A. Yi, B. Yang, Z. Wang, L. Zhou, C. Shen, Y. Zhu, Y. Zhou, R. Bao, Z. Li, Y. Chen, K. Huang, J. Zhang, Y. Cheng, and X. Ou, "High-Q microresonators on 4H-silicon-carbide-on-insulator platform for nonlinear photonics," Light: Sci. Appl. **10**(1), 139 (2021).
[33]C. Wang, J. Li, A. Yi, Z. Fang, L. Zhou, Z. Wang, R. Niu, Y. Chen, J. Zhang, Y. Cheng, J. Liu, C. H. Dong, and X. Ou, "Soliton formation and spectral translation into visible on CMOS-compatible 4H-silicon-carbide-on-insulator platform," Light: Sci. Appl. **11**(1), 341 (2022).
[34]D. V. Reddy, R. R. Nerem, S. W. Nam, R. P. Mirin, and V. B. Verma, "Superconducting nanowire single-photon detectors with 98% system detection efficiency at 1550 nm," Optica **7**(12), 1649 (2020).
[35]P. Hu, H. Li, L. You, H. Wang, Y. Xiao, J. Huang, X. Yang, W. Zhang, Z. Wang, and X. Xie, "Detecting single infrared photons toward optimal system detection efficiency," Opt. Express **28**(24), 36884 (2020).
[36]B. Korzh, Q. Y. Zhao, J. P. Allmaras, S. Frasca, T. M. Autry, E. A. Bersin, A. D. Beyer, R. M. Briggs, B. Bumble, M. Colangelo, G. M. Crouch, A. E. Dane, T. Gerrits, A. E. Lita, F. Marsili, G. Moody, C. Peña, E. Ramirez, J. D. Rezac, N. Sinclair, M. J. Stevens, A. E. Velasco, V. B. Verma, E. E. Wollman, S. Xie, D. Zhu, P. D. Hale, M. Spiropulu, K. L. Silverman, R. P. Mirin, S. W. Nam, A. G. Kozorezov, M. D. Shaw, and K. K. Berggren, "Demonstration of sub-3 ps temporal resolution with a superconducting nanowire single-photon detector," Nat. Photonics **14**, 250–255 (2020).
[37]C. Yang, M. Si, X. Zhang, A. Yu, J. Huang, Y. Pan, H. Li, L. Li, Z. Wang, S. Zhang, J. Xia, Z. Liu, H. Guo, and L. You, "Large-area TaN superconducting microwire single photon detectors for X-ray detection," Opt. Express **29**(14), 21400 (2021).
[38]V. B. Verma, B. Korzh, A. B. Walter, A. E. Lita, R. M. Briggs, M. Colangelo, Y. Zhai, E. E. Wollman, A. D. Beyer, J. P. Allmaras, H. Vora, D. Zhu, E. Schmidt, A. G. Kozorezov, K. K. Berggren, R. P. Mirin, S. W. Nam, and M. D. Shaw, "Single-photon detection in the mid-infrared up to 10 μm wavelength using tungsten silicide superconducting nanowire detectors," APL Photonics **6**(5), 56101 (2021).
[39]Y. Pan, H. Zhou, X. Zhang, H. Yu, L. Zhang, M. Si, H. Li, L. You, and Z. Wang, "Mid-infrared Nb_4N_3-based superconducting nanowire single photon detectors for wavelengths up to 10 μm," Opt. Express **30**(22), 40044 (2022).
[40]A. Al Sayem, R. Cheng, S. Wang, and H. X. Tang, "Lithium-niobate-on-insulator waveguide-integrated superconducting nanowire single-photon detectors," Appl. Phys. Lett. **116**(15), 151102 (2020).
[41]M. Si, C. Wang, C. Yang, W. Peng, L. You, Z. Li, H. Zhang, J. Huang, Y. Xiao, J. Xiong, L. Zhang, Y. Pan, X. Ou, and Z. Wang, "Superconducting NbN thin films on various (X/Y/Z-cut) lithium niobate substrates," Supercond. Sci. Technol. **35**(2), 025012 (2022).
[42]L. Yu, H. Wang, H. Li, Z. Wang, Y. Huang, L. You, and W. Zhang, "A silicon shallow-ridge waveguide integrated superconducting nanowire single photon detector towards quantum photonic circuits," Chin. Phys. Lett. **36**(8), 084202 (2019).
[43]F. Najafi, J. Mower, N. C. Harris, F. Bellei, A. Dane, C. Lee, X. Hu, P. Kharel, F. Marsili, S. Assefa, K. K. Berggren, and D. Englund, "On-chip detection of non-classical light by scalable integration of single-photon detectors," Nat. Commun. **6**, 5873 (2015).
[44]C. Schuck, X. Guo, L. Fan, X. Ma, M. Poot, and H. X. Tang, "Quantum interference in heterogeneous superconducting-photonic circuits on a silicon chip," Nat. Commun. **7**, 10352 (2016).
[45]F. Martini, A. Gaggero, F. Mattioli, and R. Leoni, "Electro-optical characterization of superconducting nanowire single-photon detectors fabricated on 3C silicon carbide," J. Low Temp. Phys. **199**(1–2), 563–568 (2020).
[46]A. Shoji, S. Kiryu, and S. Kohjiro, "Epitaxial growth of NbN and NbC_xN_{1-x} films on 3C-SiC film-covered Si wafers," IEEE Trans. Appl. Supercond. **5**(2), 2396–2399 (1995).
[47]H. W. Chang, V. K. Ranganayakulu, S. Y. Guan, P. J. Chen, M. N. Ou, Y. Y. Chen, T. M. Chuang, C. S. Chang, M. K. Wu, and M. J. Wang, "Dense rotational twins in superconducting (111)-orientated δ-NbN epitaxial films on 4H-SiC substrates," Supercond. Sci. Technol. **34**(4), 045019 (2021).